An Ultrasonic Fuel Identification System for Liquid Metal Cooled Reactors Resilient Against Multiple Transducer Failures

Dries Van Dyck and Marc Dierckx

***Abstract*—We describe a fuel assembly identification system developed for the MYRRHA reactor—a new multi-purpose flexible irradiation facility to replace the aging BR2. MYRRHA is a fast spectrum research reactor cooled with lead-bismuth eutectic (LBE) and conceived as an accelerator driven system capable of operating in sub-critical and critical modes. As liquid metal is opaque to visual light, the conventional optical fuel assembly identification system, as used by water cooled reactors, has to be replaced by a system not hindered by the opacity of the coolant. As already suggested in the late sixties, we use ultrasound for this purpose and present an encoding especially designed to enhance the robustness of the ultrasonic read-out. The encoding is based on notches of varying depth on the inflow nozzle of a fuel assembly. The depth of each notch is used to encode two bits and is measured by a dedicated transducer aligned over the notch. To increase the reliability of the fuel identification process, the identification number is protected by an error correcting code based on Hamming codes. We describe the ultrasonic system used to read out the vector of depths which is subsequently converted to a vector of bits. We explain the encoding of the twelve bit fuel identification numbers to a 22-bit error correcting code and discuss how Hamming decoding can be used to correct single bit errors, detect two bit errors or fill in the missing bits of a failing transducer. We shortly show how the confidence on the individual measurements can be taken into account using a Gaussian measurement error distribution assumption. We also present a method based on solving a linear system over Boolean variables to (partially) reconstruct the fuel identification number in case multiple transducers fail. We show that the probability on full reconstruction is 100% for up to two transducer failures, 98% for three, 79% for four and 20% for five failing transducers. Finally, we present validation results in water and lead-bismuth eutectic for the differential measurement method used to measure the depth of the notches which form the basis for the requirements of the final system which will be installed on a robotic fuel manipulator.**

***Index Terms*—Error correcting code, fuel identification, LBE, nuclear instrumentation, ultrasonic measurements.**

I. Introduction

THE idea to use ultrasonic measurement techniques as a means to identify fuel assemblies in a liquid metal cooled reactor has been around for several decades. Already in the sixties, it was mentioned by Scott *et al.* [1] as one of the 22 potential applications of ultrasound in the framework of the liquid metal fast breeder reactor development program of the United States Atomic Energy Commision (AEC). The approach considered in that era was simply to read engraved fuel identification numbers as one would do using an optical camera. Although fuel identification is mentioned in several other publications as a potential application of ultrasonic measurement techniques [2], [3], the first encoding specifically designed to enhance the robustness of the ultrasonic read-out appeared about a decade later in an article by Spanner prepared for the International Working Group on Fast Reactors [4]. Instead of trying to read an identification number, Spanner proposed to use a physical encoding composed of "coded notches and small diameter indentations placed on the top surfaces of fuel subassembly handling sockets". Although Spanner does not explain the details about the used encoding nor the rationale behind it, it is obvious that the encoding uses several depths to encode data to facilitate an ultrasonic read-out as depths can be measured reliably and precisely using time-of-flight measurements of an ultrasonic pulse.

In principle, mechanical contact-based systems could also be a basis for a fuel identification system for liquid metal cooled reactors. The main reason why we choose for a system based on ultrasound is because it is contactless and without moving parts. Minimizing the number of moving parts is an important design philosophy of MYRRHA due to concerns about the effects of LBE induced corrosion on the long term operation of moving parts.

In this article, we present a fuel identification system loosely based on the concept proposed by Spanner in 1976 in which notches of varying depth are used to encode information. In Section II, we describe the physical encoding system, the circular setup of transducers reading the code and the differential measurement technique used to measure the depth of each notch. Section III is dedicated to the error correcting code used to protect the system against measurement errors and transducer failures. First, we give a short introduction in the [7,4]-Hamming code and explain how we map a fuel identification number to the 22-bit code written on the inflow nozzle as an ordered depth sequence. We also explain how Hamming decoding can correct single bit errors, detect two bit errors or fill in the missing bits of a single transducer failure. In addition, we shortly present a method which allows to take the confidence in the individual depth measurement into account by assuming a Gaussian measurement error distribution for each transducer. Next, we show how the fuel identification number can be reconstructed, in full or partially, in case multiple transducers fail, by constructing

Manuscript received July 03, 2013; revised December 05, 2013; accepted January 31, 2014.

The authors are with SCK-CEN, Belgian Nuclear Research Centre, BE-2400, Mol, Belgium (e-mail: dries.van.dyck@sckcen.be; marc.dierckx@sckcen.be).

Digital Object Identifier 10.1109/TNS.2014.2304753

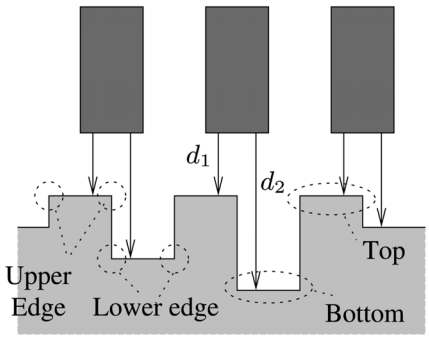

Fig. 1. Differential measurement: the depth of a notch is measured by taking the difference $d_2 - d_1$ between the distance to the top d_1 (first echo) and bottom of a notch d_2 (second echo), as shown for the transducer in the middle.

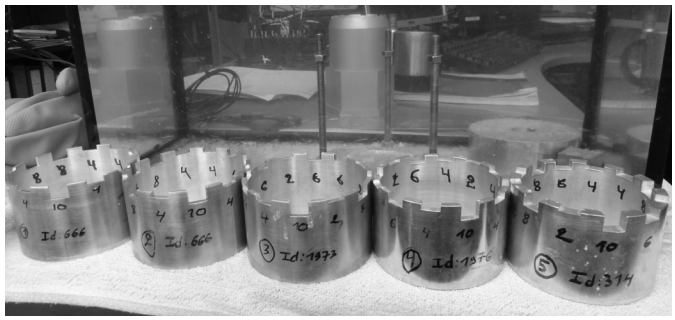

Fig. 2. Fuel identification mockups.

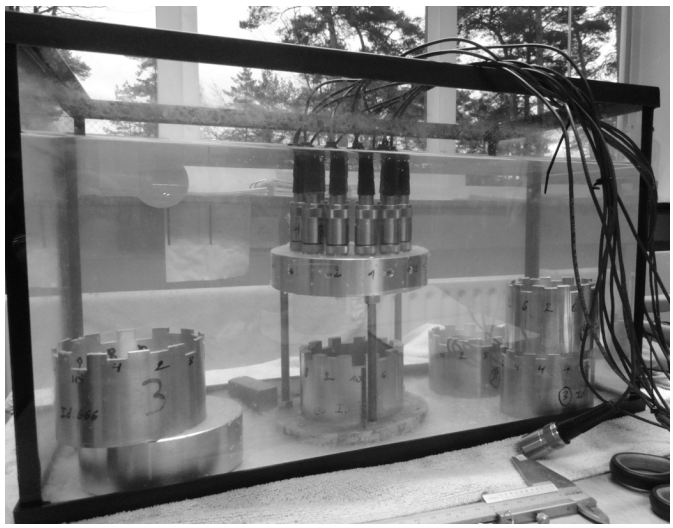

Fig. 3. Measurement setup in small water pool to position the twelve transducers above a mockup.

and solving a linear system over Boolean variables. We show that error detection is no longer guaranteed in case of a double transducer failure but that the identification number can be correctly reconstructed if the remaining data is correct. We also deduce that the probability on full reconstruction is about 98% for three, 79% for four and 20% for five failing transducers. In Section IV, we present validation results of the differential measurement method in water which demarcate the alignment requirements for the final system to be installed on the robotic fuel manipulator of MYRRHA [5]. In Section V we discuss some first results from the ongoing validation in LBE. Finally, we summarize our conclusions in Section VI.

II. The Fuel Identification System

As a conventional optical read-out of a fuel identification number is impossible due to the opacity of the coolant, MYRRHA will use an ultrasonic system to identify fuel. The idea is to encode an identifier on the inflow nozzle of a fuel assembly by means of a series of notches of varying depth. The depth of the notch is used to encode information and each notch encodes two bits–*a quad*–according to the table below:

depth [mm]	2	4	6	8
quad (= 2 bits)	00	01	11	10

By using quads instead of the conventional bits, we can halve the number of notches and thus the number of transducers required to read the code. Remark that we ordered the two bit sequences in such a way that misreading a depth level of 2 mm always leads to a single and not a two bit error.

The depth of the notch itself is determined by what we call *differential measurement*. We position a transducer over the edge of the notch such that two reflections can be received from a single pulse: one from the top and one from the bottom of the notch, as illustrated in Fig. 1. The depth of the notch is then determined by taking the difference between these two time-of-flight measurements and translating the result to distance using the known speed of sound of the medium.

Analysis of the possible fuel management schemes of MYRRHA lead us to the conclusion that about 2400 identifiers suffice for 60 years of operation, which requires twelve bits ($2^{12} = 4096$). As the long term reliability of ultrasonic transducers submerged in hot LBE is unknown, we decided to protect the identification number with an error correcting code based on the well known Hamming code [6]. The result is a 22-bit or 11-quad code which will be written on the inflow nozzle. The mapping from 12-bit identification number to the 22-bit code will be explained in detail in the following section.

Fig. 2 shows five mockups of variable mantle thickness we used to validate the fuel identification system in water. Each mockup contains twelve notches: eleven notches comprising the physical encoding of the error correcting code of the fuel identification number and one so-called *border notch*: an additional notch of 10 mm depth which could be used to determine the orientation of the mockup. In the remainder of this article, we assume that the orientation of the fuel assembly is known through a locking mechanism used by the robotic fuel manipulator and does not need to be determined via ultrasonic means.

The code is read by a circular setup of twelve transducers—a dedicated transducer for each notch aligned above the edge of the notch. Fig. 3 shows the measurement setup composed of a circular disk holding the transducers supported by three nutbolts on threaded rods and a mockup holder below.

III. The Error Correcting Code

A. Introduction and Main Principles Error Correcting Code

In order to increase the reliability of the fuel identification process, the identification number is protected by an error correcting code. The error correcting code is composed of three interleaved, carefully permuted [7,4]-Hamming code words enriched with an overall parity bit to increase our reconstructive capabilities in case of multiple transducer failures. The result is a code which is capable of correcting all single bit errors and detecting all two bit errors at unknown locations. In addition, thanks to the interleaving principle, it also corrects a two bit error caused by a single transducer at an unknown position.

Transducer failures give rise to a code with missing bits at known locations. The knowledge of the locations of the missing bits allows reconstruction by solving a linear system over Boolean variables. Depending on the number of missing bits and their locations, there are in essence three possible outcomes:

1) full reconstruction with limited error detection
2) full reconstruction without error detection; and
3) partial reconstruction with generation of all possible identification numbers consistent with the data.

The remainder of this section is organized as follows. We first give a short introduction in the [7,4]-Hamming code. Next, we explain the mapping from the 12-bit identification number to the 22-bit error correcting code and discuss the basic error correcting capabilities which follow immediately from Hamming encoding and the interleaving principle. We also describe how the confidence in individual measurements can be taken into account using a Gaussian error distribution assumption. Finally, we explain how we can (partially) reconstruct the identification number if more transducers fail than simple Hamming code correction can handle.

In the rest of this section, we assume that the reader is familiar with basic linear algebra.

B. The [7,4] Hamming Code

We will first refresh how Hamming codes are normally used: to detect up to two bit errors or to correct a single bit error at unknown locations [6]. Let u be a 4-bit data vector.

In the [7,4]-Hamming code, we map a 4-bit data vector u to a 7-bit vector v by appending the parity of three 3-bit subsequences of the original 4-bit data vector u:

$$[7,4] : u = (x_1x_2x_3x_4) \rightarrow (x_1x_2x_3x_4(x_2 \oplus x_3 \oplus x_4)(x_1 \oplus x_3 \oplus x_4)(x_1 \oplus x_2 \oplus x_4)) = v \quad (1)$$

where $\oplus$ stands for the exclusive OR binary operator (XOR or equivalenty the sum modulo 2). The resulting 7-bit vector v is called a *code word*.

Hamming codes are linear codes. In a linear code, the mapping of k-bit data vector u to its n-bit code word v is achieved by multiplying it with a so called *generator matrix* G of dimension $k \times n$, i.e.

$$v = E(u) = uG. \quad (2)$$

In our case, $n = 7$ and $k = 3$.

Once a code v is read, it can be verified by multiplying it with the so called *parity check matrix* H of dimension $(n-k) \times n$. If v is indeed a code word obtained by encoding some u, this multiplication equals the zero vector:

$$vH^T = 0_{(n-k)} \Leftrightarrow \exists u : v = E(u) \quad (3)$$

For Hamming codes $n = 2^r - 1$, $k = 2^r - r - 1$ which makes $n - k = r$. For our [7,4] code, $r = 3$ and we have:

$$G = \begin{pmatrix} 1 & 0 & 0 & 0 & 0 & 1 & 1 \\ 0 & 1 & 0 & 0 & 1 & 0 & 1 \\ 0 & 0 & 1 & 0 & 1 & 1 & 0 \\ 0 & 0 & 0 & 1 & 1 & 1 & 1 \end{pmatrix} \quad (4)$$

and

$$H = \begin{pmatrix} 0 & 0 & 0 & 1 & 1 & 1 & 1 \\ 0 & 1 & 1 & 0 & 0 & 1 & 1 \\ 1 & 0 & 1 & 0 & 1 & 0 & 1 \end{pmatrix} \quad (5)$$

Remark the special structure of the parity check matrix: column i is simply the binary representation of i when read from bottom to top.

If $vH^T = z \neq 0_3$ then z equals the binary representation of the index of the bit that must be flipped to obtain the closest valid code word. This is easy to see. Let v be the correct code word and $v' = v \oplus e$ the same code with some error vector e added to it, we get with equation (3):

$$v'H^T = (v \oplus e)H^T = vH^T \oplus eH^T = eH^T.$$

If e contains a single bit error, say at position i, then $eH^T = H_i^T$, with H_i the ith column of H. By construction, H_i equals the binary representation of i.

On the other hand, if e contains more than one bit error, than we have two possible outcomes. Either v' is an other valid code word and the bit errors pass undetected as $v'H^T = 0_3$ or v' is not a valid code word and Hamming decoding transforms v' to the closest codeword by flipping the wrong bit, which is not the encoding of the original data. It is a known property of Hamming codes that at least three bits must be flipped to change a valid code word v into an other valid code word v'. Therefore, a two bit error will be noticed as $v'H^T \neq 0_3$ but Hamming decoding will flip the wrong bit and the result will not be the encoding of the original data. Remark that in that case, we end up with a code word that differs in exactly three bits from the original and thus also in parity, which will be noticed by the overall parity bit we add to the three Hamming code words as explained in next subsection.

C. From Identification Number to Error Correcting Code

In order to apply [7,4]-Hamming encoding, we first split the 12-bit identification number into three 4-bit vectors a, b and c which are then encoded by multiplying them with G as in equation (2). As Hamming encoding is performed on a row-basis, it is convenient to write it as a matrix multiplication:

$$\begin{pmatrix} a \\ b \\ c \end{pmatrix} G = \left(\begin{array}{cccc|ccc} a_1 & a_2 & a_3 & a_4 & a_5 & a_6 & a_7 \\ b_1 & b_2 & b_3 & b_4 & b_5 & b_6 & b_7 \\ c_1 & c_2 & c_3 & c_4 & c_5 & c_6 & c_7 \end{array}\right) \quad (6)$$

where the elements to the right of the marker line are the bits added by Hamming encoding. Next, we apply a permutation to make sure that the linear relations introduced by Hamming encoding are distributed over the different transducers[1]: we permute bG by reversing it and cG by shifting it circularly two positions to the right, to obtain:

$$\begin{pmatrix} a_1 & a_2 & a_3 & a_4 & a_5 & a_6 & a_7 \\ b_7 & b_6 & b_5 & b_4 & b_3 & b_2 & b_1 \\ c_6 & c_7 & c_1 & c_2 & c_3 & c_4 & c_5 \end{pmatrix}. \quad (7)$$

Finally, we interleave the codewords by flattening the matrix above columnwise to make sure that two bits of a same quad are always from different codewords and add an overall parity bit $p = \sum_{i=1}^{7}(a_i \oplus b_i \oplus c_i)$ to obtain the final 22-bit code:

$$(a_1 b_7\, c_6 a_2\, b_6 c_7\, a_3 b_5\, c_1 a_4\, b_4 c_2\, a_5 b_3\, c_3 a_6\, b_2 c_4\, a_7 b_1\, c_5 p) \quad (8)$$

Remark that the two bits read-out by the same transducer, those without a separating space in equation (8), are from different code words and have a different position within a codeword.

Thanks to the interleaving principle, a two bit error caused by a same transducer, can always be corrected directly by Hamming decoding as it results in two single bit errors in different code words. Of course, two lost bits due to a single transducer failure can be handled as a two bit error by assigning them arbitrary values and let Hamming decoding correct them if necessary.

D. Using Confidence Model Individual Depth Measurements

Simple Hamming decoding transforms an invalid code word v' into that valid code word having the most bits in common with v'. In the pure binary setting this is the logical approach, but in our setting we can also use information present in the vector of depth measurements which was translated into bits. Indeed, our confidence in the correctness of a bit depends on the deviation of the depth corresponding to a quad with this bit value. E.g., when measuring 4.8 mm, our confidence in the first bit of the quad is much less than in the second as the quads corresponding to the depth level 4 mm and 6 mm agree on the second bit but differ on the first bit.

[1]In fact, the permutation does something stronger: it maximizes the probability on full reconstruction when more than two transducers fail as will be explained at the end of this section.

Let Δ be the vector of deviations between the measured depths of the notches and the ideal depth vector encoding an identification number, i.e., without measurement errors. If we assume that the individual measurement errors of each of the transducers follow a Gaussian distribution and are identically and independently distributed, the probability of getting a measurement error vector Δ is proportional to:

$$P(\Delta) = \prod_{i=1}^{11} e^{-\frac{(\Delta-\mu_i)^2}{2\rho_i^2}}. \quad (9)$$

The choice of μ_i and ρ_i can be adapted to the calibration data of the transducers. For instance, with $\mu_1 = 0$ and $\rho_1 = 0.3$, we express that we expect the measurement error of the first transducer is for 68.2% of the cases within $\pm\rho = \pm 0.3$ mm and 95.4% within $\pm 2\rho = \pm 0.6$ mm.

Calculating Δ for code words in the larger neighborhood of v' and evaluating equation (9) allows to not only consider the closest but also the most likely correct code word taking into account calibration data of the individual transducers and the continous nature of the depth measurements.

E. Reconstruction in Case of Multiple Failing Transducers

In case multiple transducers fail, simple Hamming decoding no longer suffices to fill in the missing bits and we have to exploit the knowledge of the location of the missing bits. This is achieved by handling the missing bits as variables in a linear system over Boolean variables and solve the system. The fact that this approach is valid with Boolean variables and the XOR-operator $\oplus$ follows from the fact that the XOR-operator is equivalent with the sum modulo two. It is well known from the theory of finite fields [7] that all properties of a field required to solve a linear system such as commutativity, associativity and distributivity remain valid when calculating modulo a prime number.

For ease of presentation, we first explain how such a linear system is constructed on the level of a single Hamming code word for three missing bits. To that end, we transform equation (3) into a linear system by first replacing the missing bits by variables y_1, y_2 and y_3 and then performing the multiplication Hv^T. The result gives us a vector with an expression in terms of the variables y_i and some constants which should equal the zero vector, according to equation (3). Hence, we obtain a linear system with three equations in three variables. For instance, if we loose bit 1, 3 and 5 of $v = (\underline{1}0\underline{1}1\underline{0}10) = E((1011))$, we get by equation (3):

$$\begin{pmatrix} 0 & 0 & 0 & 1 & 1 & 1 & 1 \\ 0 & 1 & 1 & 0 & 0 & 1 & 1 \\ 1 & 0 & 1 & 0 & 1 & 0 & 1 \end{pmatrix} \begin{pmatrix} y_1 \\ 0 \\ y_2 \\ 1 \\ y_3 \\ 1 \\ 0 \end{pmatrix} = \begin{pmatrix} 0 \\ 0 \\ 0 \end{pmatrix}$$

$$\Leftrightarrow \begin{pmatrix} 0 & 0 & 1 \\ 0 & 1 & 0 \\ 1 & 1 & 1 \end{pmatrix} \begin{pmatrix} y_1 \\ y_2 \\ y_3 \end{pmatrix} = \begin{pmatrix} 0 \\ 1 \\ 0 \end{pmatrix}$$

A little thought will show that we can transfrom equation (3) directly into the well known $Ay = b$ form by doing the following vector matrix operations. We first remove the columns from H which correspond to the known bits. This gives us A—the coefficients of y_1, y_2 and y_3 in the linear system of equations. Next, we construct b, the vector of constants forming the right hand side of the system. To that end, we first remove the columns which correspond to the unknown bits from H, call the result H_{known}. Then we remove the unknown bits from v, call the result v_{known}. We can now calculate $-b = H_{\text{known}} v_{\text{known}}^T = b$ because we calculate modulo 2. Finally, we can use efficient algorithms such as Gaussian elimination to solve the $Ay = b$ linear system we just constructed.

If we apply the same principle to the complete code with an arbitrary number of missing bits, we obtain ten equations in total: three times three equations of the three Hamming code words and an additional equation from the parity bit spanning over all three Hamming code words. As the overall parity bit is the only equation containing bits of all Hamming code words, this linear system will have the following structure:

$$\left(\begin{array}{c|c|c} A^1_{l_1\times m_1} & 0_{l_1\times m_2} & 0_{l_1\times m_3} \\ \hline 0_{l_2\times m_1} & A^2_{l_2\times m_2} & 0_{l_2\times m_3} \\ \hline 0_{l_3\times m_1} & 0_{l_3\times m_2} & A^3_{l_3\times m_3} \\ \hline 1_{1\times m_1} & 1_{1\times m_2} & 1_{1\times m_3} \end{array}\right) \left(\begin{array}{c} y^1 \\ \hline y^2 \\ \hline y^3 \end{array}\right) = \left(\begin{array}{c} b^1 \\ \hline b^2 \\ \hline b^3 \\ \hline p' \end{array}\right), \quad (10)$$

with l_i the number of equations and m_i the number of variables in the linear system $A^i y^i = b^i$ induced by the missing bits of Hamming code word i, and p' the constant obtained from summing all known bits, including the parity bit.

Of course, before we try to solve the linear system, we have to check whether the number of independent equations is greater or equal than the number of variables. That is, we have to compare the *rank* of A with the number of variables. In addition, if the number of equations exceeds $\text{rank}(A)$, we have to check their consistency. Let $l = 1 + \sum_{i=1}^{3} l_i$ be the number of equations and $m = \sum_{i=1}^{3} m_i$ the number of variables of equation (10). We consider four possible cases:

1) $l = m = \text{rank}(A)$: The system has a unique solution.
2) $l > m \geq \text{rank}(A)$: The system is overdetermined and possibly inconsistent. If it is consistent, it has a unique solution, otherwise it has no solution. We can solve it by removing dependent equations until the number of equations equals the rank. Afterwards, we can check the consistency of the system by checking if the solution also adheres the removed equations.
3) $m > l \geq \text{rank}(A)$: The system is underdetermined and has multiple solutions. Because we work binary, we can generate a finite set of solutions by considering the two possible values of a variable, adapt the vector of constants b accordingly and recursively try to solve the system with $m - 1$ variables until we eventually obtain a system with an unique solution. This will yield $2^{m-\text{rank}(A)}$ possible solutions for the linear system—one for each combination to fix the variables.
4) $l = m > \text{rank}(A)$: The system is dependent and as the number of equations is larger than the rank, possibly inconsistent. Removing a dependent equation reduces it to previous case ($m > l$) but after solving the system, its consistency has to be checked by checking if the solutions adhere the removed independent equation.

Checking the consistency of an overdetermined linear system is the only way left to detect errors as soon as information is lost.

The reason why we applied a permutation on the three Hamming code words in equation (6), is to minimize the number of dependent systems in equation (10) if more than two transducers fail. If two transducers fail, we have four missing bits of which at most two in a single Hamming code word and there are always at least two independent equations from Hamming encoding. If three transducers fail, we can loose two times three bits in a single Hamming code word but thanks to the permutation we introduced, at most one has dependent equations which can be compensated by the equation from the parity bit, unless we also lost the parity bit. The table below summarizes the probability on full reconstruction of the code in function of the number of failing transducers:

Nr Failing Transducers	3	4	5
Nr independent systems	162	260	92
Nr combinations	165	330	462
P(full reconstruction)	98.18%	78.79%	19.91%

To put these results in perspective: the same error correcting code but without bit permutation and overall parity bit, results in probability on full reconstruction of 87% for three, 47% for four and 5% for five failing transducers.

IV. Validation of Differential Measurement in Water

In order to demarcate the main requirements for the physcial encoding on the mantle of the inflow nozzle and the robotic fuel manipulator to read out the code reliably, we set up a validation experiment in water. Using the setup shown in Fig. 3 with twelve 5 MHz transducers in the transducer ring, we read out several aluminium mockups with a mantle thickness of 2.5 mm, 4.0 mm, 5.0 mm and 7.5 mm, see Fig. 2, from several stand-off distances and in several alignment conditions. To differentially measure the depth of the notches, the robotic fuel manipulator must grab and lock the fuel assembly and align itself with the inflow nozzle such that the transducers are correctly aligned above the notches. By *parallel* alignment, we mean that the transducer ring should be parallel with the plane defined by the top of the notches in order to aim the transducers perpendicularly at the notches. In practice, parallel alignment will not be perfect. In that case, we say that the transducer ring is *tilted* and call the angle between the transducer ring plane and the plane defined by the top of the notches the *tilt angle* θ. By an *azimuthal angle* φ, we refer to an angle in the plane of the transducer ring, with respect to the lowest point on the transducer ring when it is tilted.

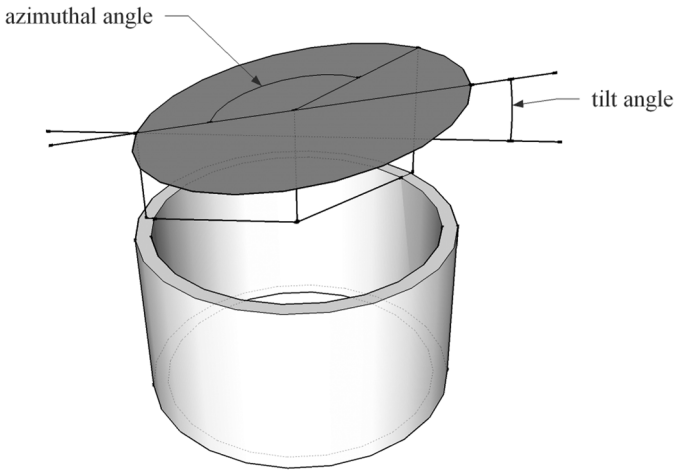

Fig. 4. Illustration of the tilt and azimuthal angle. The cylinder below represents the mockup and the disk above it the ring containing the transducers.

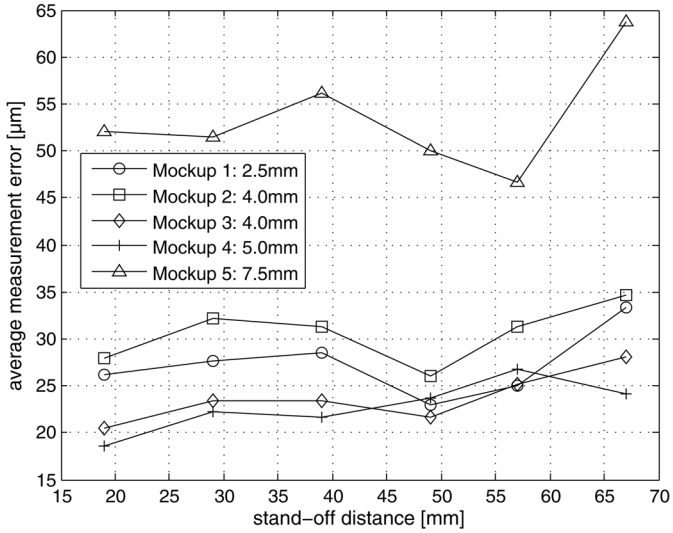

Fig. 5. Average measurement error in function of distance for each mockup.

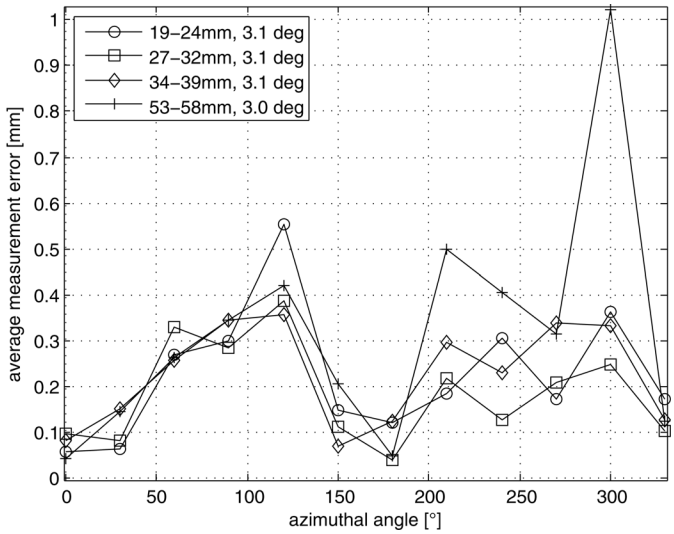

Fig. 6. Measurement error under a tilt angle in function of the azimuthal angle of the transducer at different distances.

We will use the azimuthal angle to refer to the position of a transducer when the transducer ring is tilted. Both the tilt angle θ and azimuthal angle φ are illustrated in Fig. 4.

The tilt angle θ can be simulated by changing the height of the nutbolts on the threaded rods. The nutbolts are also used to change the measurement distance.

The differential measurement itself is performed by taking the maximum values of the two strongest peaks from the time traces sampled at 100 MHz after improving the signal to noise ratio using a matched filter—or equivalently auto-correlation, see e.g. [8]—and transforming the multiple peaks of a single reflected pulse to a single dominant peak by taking the amplitude envelope using the Hilbert transform [9].

First, we determined the minimal distance for a reliable measurement which is dependent on two factors: the time required to let the transducer come to rest and start receiving and to rule out ambiguity between primary and secondary reflections. The latter issue arises when a pulse hits the transducer face a second time after traveling the path between transducer and target twice (or more) and still arrive at a time consistent with a primary reflection. More formally, if the transducer measures at a distance d_1 from the top and a distance d_2 from the bottom of a notch, we can expect secondary "ghost" reflections at integer linear combinations of d_1 and d_2, i.e., at distances $ad_1 + bd_2$, for natural numbers a and b. Of course, in practice, the main concern is the secondary reflection from the top of the notch at $2d_1$ which could overpower the reflection from the bottom at d_2 if the transducer is not well aligned above the notch. We did indeed observe such a secondary reflection at $2d_1$, which was stronger than the one at d_2 and only deviated 0.2 mm from a valid depth which is well with the expected measurement error of a wavelength $\lambda = 0.3$ mm when measuring from a stand-off distance of 3.8 mm. Several other weaker secondary reflections were also observed but only the one at $2d_1$ can be considered problematic. In conclusion, it is better to avoid this ambiguity by using a stand-off distance such that $2d_1 \gg d_2$ for any possible d_2. As the maximum value of $d_2 - d_1$ is 10 mm, a stand-off distance of 15 mm suffices, which is also sufficient to start reception without being hindered by the residual oscillation from transmission.

Next, we looked at the measurement error in function of distance when measuring perfectly perpendicular. The result are graphically depicted in Fig. 5. Except for the thickest mockup of 7.5 mm, the average measurement error is relatively stable over the complete distance region considered and seems to be independent of thickness: about a quarter of a wavelength for the thickest mockup and about a tenth of a wavelength for the others, but of course under ideal conditions.

When measuring under a tilt angle θ, the azimuthal angle φ between the transducer and the lowest point of the transducer ring (see Fig. 4) with respect to the mockup becomes important. Fig. 6 shows a plot of the measurement error in function of azimuthal angle for a variety of stand-off distances and tilt angle combinations.

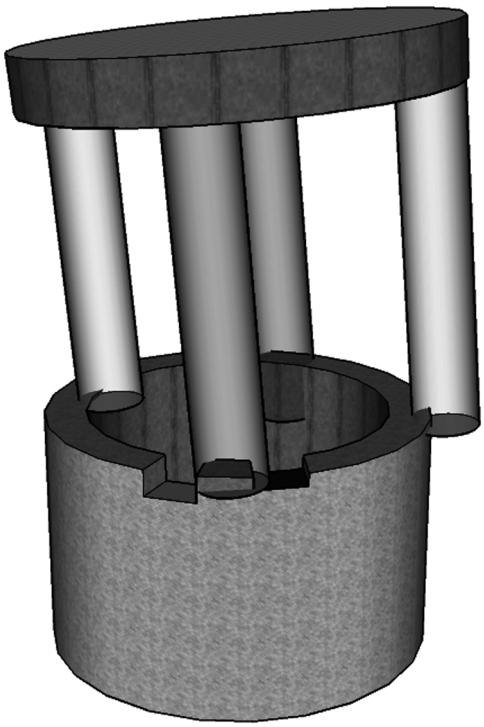

Fig. 7. Illustration showing the movement of the ultrasonic beam under a large tilt angle. The light and dark cylinders represent ultrasonic beams. The light beams move radially ($\varphi \in \{0, 180\}^\circ$) while the dark beams move tangentially ($\varphi = \pm 90^\circ$). The dark beam in front should measure the notch with the grey bottom, but due to the large tilt angle, the ultrasonic spot overlaps more with the neighboring notch with the black bottom.

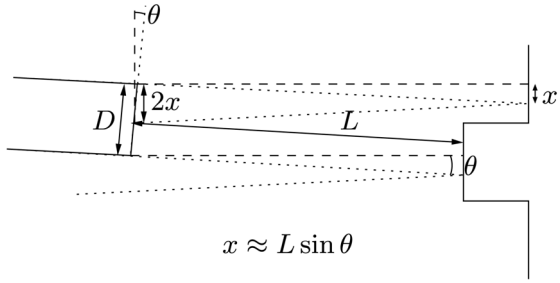

Fig. 8. A transducer that differentially measures a notch under a tilt angle θ from a distance L. Its ultrasonic spot moves $x \approx L \sin\theta$ in the tilt direction.

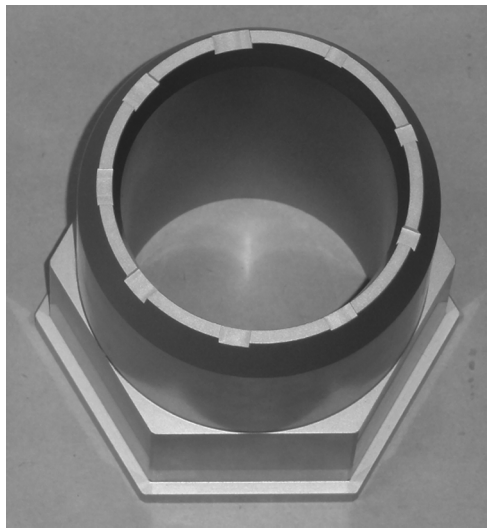

Fig. 9. Stainless steel mockup of a fuel assembly inflow nozzle containing notches of depth 1 mm, 2 mm and 3 mm and width 10 mm, 5 mm and 8 mm.

By construction of the experimental setup, we can only create a tilt angle by rotating the transducer ring around a line close to the center of the transducer ring—the center of the disk in Fig. 4. Due to rotating the transducer ring around a line through its center, the ultrasonic spot of all transducers will move in the direction defined by the line from lowest to highest point of the transducer ring. This means that for transducers with an azimuthal angle φ close to $\pm 90°$, the ultrasonic spot will move mostly tangential to the cylindric mantle of the mockup, while for those close to 0 or 180°, the movement is mostly radial to the cylindric mantle, as illustrated in Fig. 7. Especially for the notches where the movement is mostly tangential, the distribution of acoustic energy is no longer evenly distributed over the top and bottom of notch and under larger tilt angles it is even possible to get a stronger reflection from the bottom of a neighbouring notch instead of the intended notch. In addition, the reflection we get from notches with an azimuthal angle close to $\pm 90°$ is a reflection from a slope as the tilt angle is in the direction of the length of the notch.

A simple 2D-model assuming that the tilt angle is a result of rotating the transducer around a line trough the center of the transducer face already gives an idea of how much the ultrasonic spot can move with the experimental setup we used. If we model the beam as a perfect cylinder with a diameter equal to the transducer diameter and assume that the transducer is tilted in a plane parallel with the notch, a 2D-cut would look like Fig. 8. This situation is geometrically similar to the situation of the transducer which is at an azimuthal angle of $-90°$. Remark that the length of the notch and the space in between the notches is about the same as the diameter of a transducer. From Fig. 8 it follows that as soon as $x > D/2$, more acoustic energy will hit the bottom of the neighboring notch than the bottom of the intended notch. Using our approximation this would mean that this happens as soon as

$$\sin\theta > \frac{D}{2L} \Leftrightarrow \theta > \arcsin\left(\frac{D}{2L}\right) \tag{11}$$

As a practical rule of thumb, a conservative limit is to keep $x \leq D/5$ which corresponds to 25% of the ultrasonic energy if the energy is evenly distributed over a circular ultrasonic spot. The table below lists the maximal tilt angle θ to adhere to this condition for a given measurement distance d_1:

d_1 [mm]	15	20	25	30	35	40	45	50	55	60	65	70
θ[°]	9.6	7.2	5.7	4.8	4.1	3.6	3.2	2.9	2.6	2.4	2.2	2.0

V. Validation in LBE

As most results from the validation in water can be extrapolated to LBE thanks to the similar speed of sound in both liq-

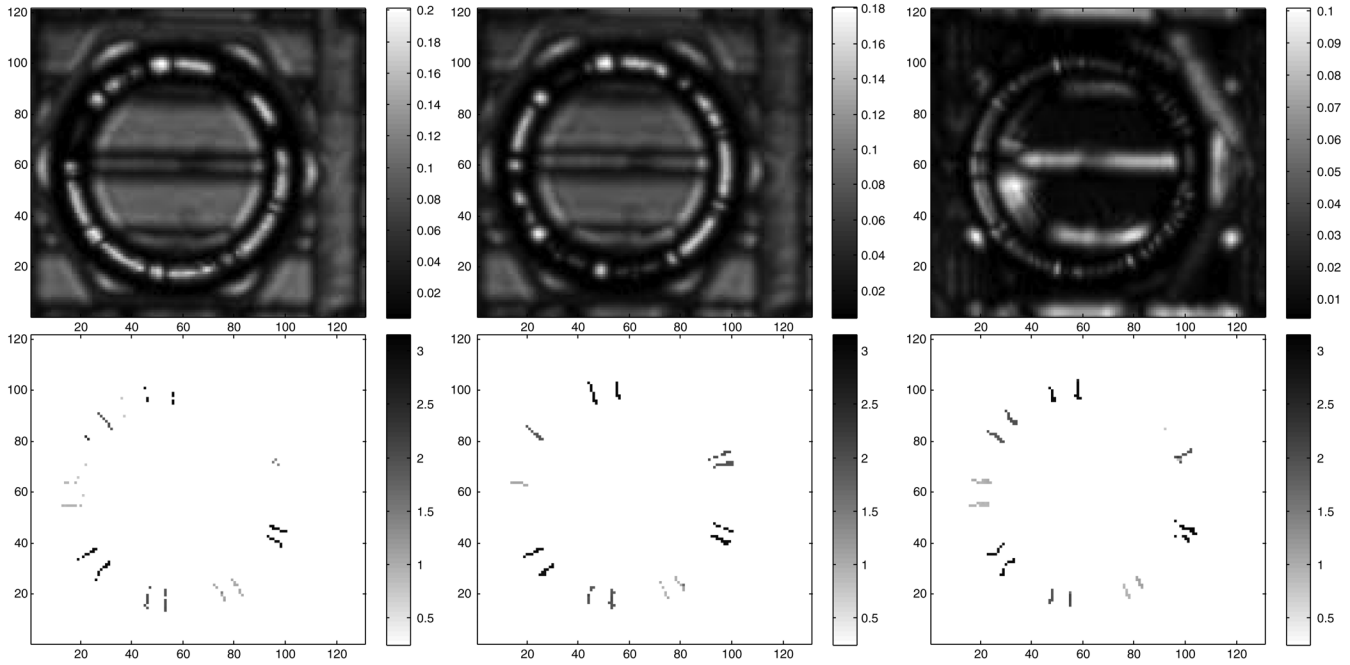

Fig. 10. C-scans of the mockup depicted in Fig 9 from stand-off distances $d_1 = 35$ mm (left), $d_1 = 70$ mm (middle), $d_1 = 77 \rightarrow 83$ mm, $\theta = 3^\circ$ (right). **Top**: Amplitude strongest reflection. **Bottom**: Differential measurements between two strongest reflections p_1 and p_2 restricted to the interval [0.75,3.25].

uids [10], we are mostly interested in the measurement error of differential measurement using a radiation hard, LBE-compatible, high temperature transducer. The transducer we employed has a bismuth-titanate piezo electric ceramic of 8 mm diameter and a center-frequency of 5 MHz. For more details on the used transducer, we refer to an other publication by the same authors where we dedicate a short section to transducer design [11].

For a first validation in LBE, we performed a C-scan of a stainless steel mockup of the inflow nozzle of a fuel assembly shown in Fig. 9. The mockup contains three groups of three notches with a 1 mm, 2 mm and 3 mm deep notch in each group. Starting clockwise from the leftmost notch, we first have a group with a width of 10 mm, followed by a group of width 5 mm and finally a group of width 8 mm.

Fig. 10 shows the amplitude and the results from applying differential measurement on the C-scans in LBE. Differential measurement was applied in the same way as in water but restricted to those positions where the result is within the interval [0.75,3.25] and the ratio $p_2/p_1 \geq 0.5$, with p_1 and p_2 the amplitudes of the two strongest reflections ($p_1 \geq p_2$) which should be from the top and bottom of the notch. The measurement with tilt angle is also a C-scan but with the scenery tilted by $\theta = 3^\circ$ from which we picked the best reflections for differential measurement and can therefore not be compared with the much more stringent tilted measurements in water using only a single measurement at a fixed position.

As one can see, the reflective properties of stainless steel change during the scan—see [10] for an in depth discussion. Before the scan, we stirred the LBE resulting in reasonably good reflections in the first scanning positions, from left to right in Fig. 10: the lower, right and left part of the scan. After some time, the signal detoriates and some gas bubbles appear to stick to the stainless steel. Identification of the root cause of this behavior is a main research track for the near future. Nevertheless, rudimentary analysis of differential measurement results on the good parts of the scans indicated subwavelength precision (0.35 mm) for the 2 mm and 3 mm notches, even when tilted.

For the 1 mm notches, the smaller bandwidth of the high temperature transducer resulted in overlap of the top and bottom reflection which often required some tweaking of the matched filter to separate both peaks. Although we do not use 1 mm notches in the encoding from Section II and no such problems were observed for the deeper notches, it might be prudent to make all notches 1 mm to 2 mm deeper.

VI. Conclusion

We described a fuel identification system based on measuring the depth of notches, each of which encodes two bits of an error correcting code containing the fuel identification number. The depth of each notch is measured by a dedicated transducer aligned over the edge of notch which allows to determine two distances in a single measurement: the distance to the top and to the bottom of the notch. The depth is then determined by taking the difference between these distances.

We also explained the mapping from the twelve bit identification number to the 22-bit error correcting code based on three interleaved, carefully permuted [7,4]-Hamming code words enriched with an overal parity bit and showed that with this code we can correct any single bit error and any single quad error directly by using Hamming decoding. We presented a method to take the confidence on the individual depth measurements into account by assuming that the individual transducers follow a

Gaussian distribution which can be constantly adapted by transducer calibration data.

As the long term behavior of transducers in LBE under reactor conditions is unknown, we also investigated with what probability a fuel identification number can be reconstructed if a certain number of transducers fail. Thanks to the knowledge of the locations of the missing bits, reconstruction is possible by considering the missing bits as variables in a linear system over Boolean variables in which the equations are the linear relations introduced by the error correcting code. Thanks to the well chosen permutation of the Hamming code words and the extra overall parity bit, we can minimize the number of linear systems in which the number variables exceeds the number of independent equations. In that way, we can guarantee reconstruction if less than three transducers fail and have a probability on full reconstruction of 98% for three, 79% for four and 20% for five failing transducers.

Finally, we presented the main results of a thorough validation of the fuel identification system and the differential measurement method in water and first validation results from the ongoing validation in LBE.

Foremost, the validation in water showed that we can reliably read out the fuel identification code from any stand-off distance within the limitations imposed by the experimental setup. The lower limit is mainly to avoid ambiguity between primary reflections from the bottom and secondary reflections from the top. The thickness of the mockups played no significant role in any of the problems observed. Hence, any thickness between 2.5 mm and 7.5 mm for the mantle containing the notches will be fine. The precision of differential measurement is strongly dependent on the combination of tilt angle and stand-off distance. When measuring perpendicularly, the precision is better than half a wavelength (0.15 mm) for any distance considered but the more we tilt the transducer ring, the closer we need to measure to catch enough of the strong specular reflection. For tilt angles below 3°, identification is flawless at all stand-off distances and the measurement precision is about two wavelengths (0.75 mm).

Although validation of differential measurement in LBE is still ongoing, results from the initial parts of the C-scans are promising and indicate no strong deviation from the non-restrictive requirements which follow from the validation in water. That being said, the reason for the deterioration of the reflected signals over time need to identified in future research.

ACKNOWLEDGMENT

The authors would like to thank colleagues Ludo Vermeeren and Willem Leysen for constructive comments on an earlier version of this paper and technicians Johny Mols, Jean Pouders, and Stan Van Ierschot for valuable technical assistance with setting up the experiments.

REFERENCES

[1] C. C. Scott, P. R. Huebotter, and R. C. Callen, Potential applications for an under-sodium ultrasonic scanning device, Atomic Power Development Associates Report, Tech. Rep., Jul. 1967.

[2] C. K. Day and R. W. Smith, "Under-sodium viewing," in *Proc. IEEE Ultrasonics Symp.*, Monterey, CA, USA, Nov. 1974.

[3] R. N. Ord and R. W. Smith, Development of an under-sodium ultrasonic scanner for in-reactor surveillance Hanford Engineering Development Laboratory, Tech. Rep. HEDL-TME 72–91, Jun. 1972.

[4] J. C. Spanner, "Preliminary development of inservice inspection methods for LMFBR's," in *Proc. International Working Group on Fast Reactors Specialists Meeting on "Inservice Inspection and Monitoring of LMFBR's"*, Bensberg, Germany, Mar. 1976.

[5] H. Aït Abderrahim and P. D'Hondt, "MYRRHA status at mid-2005 and prospective towards implementation: A european experimental ADS for R&D applications," *J. Nucl. Sci. Technol.*, vol. 44, no. 3, pp. 491–498, 2007.

[6] R. W. Hamming, "Error detecting and error correcting codes," *Bell Syst. Tech. J.*, vol. 29, no. 2, pp. 147–160, 1950.

[7] R. Lidl and H. Niederreiter, *Introduction to finite fields and their applications*. Cambridge, MA, USA: Cambridge Univ. Press, 1996.

[8] W. S. Burdic, *Underwater Acoustic Systems Analysis*. Englewood Cliffs, NJ, USA: Prentice Hall, 1991.

[9] R. G. Lyons, *Understanding Digital Signal Processing (Third Edition)*. Upper Saddle River, NJ, USA: Prentice Hall, 2010.

[10] M. Dierckx and D. Van Dyck, "Research towards ultrasonic systems to assist in-vessel manipulations in liquid metal cooled reactors," presented at the Advancements in Nuclear Instrumentation Measurement Methods and their Applications (ANIMMA) Conf., Marseille, France, Jun. 2013.

[11] M. Dierckx and D. Van Dyck, "Research towards ultrasonic systems to assist in-vessel manipulations in liquid metal cooled reactors," *IEEE Trans. Nucl. Sci.*, accepted for publication.